EMBO reports

scientific report

The *mbk-2* kinase is required for inactivation of MEI-1/katanin in the one-cell *Caenorhabditis elegans* embryo

Sophie Quintin[1], *Paul E. Mains*[2], *Andrea Zinke*[1] & *Anthony A. Hyman*[1+]

[1]Max-Planck-Institute of Molecular Cell Biology and Genetics, Pfotenhauerstrasse, Dresden, Germany, and [2]Genes and Development Research Group, Department of Biochemistry & Molecular Biology, University of Calgary, Calgary, Alberta, Canada

The *Caenorhabditis elegans* early embryo is widely used to study the regulation of microtubule-related processes. In a screen for mutants affecting the first cell division, we isolated a temperature-sensitive mutation affecting pronuclear migration and spindle positioning, phenotypes typically linked to microtubule or centrosome defects. In the mutant, microtubules are shorter and chromosome segregation is impaired, while centrosome organization appears normal. The mutation corresponds to a strong loss of function in *mbk-2*, a conserved serine/threonine kinase. The microtubule-related defects are due to the post-meiotic persistence of MEI-1, a homologue of the microtubule-severing protein katanin. In addition, P-granule distribution is abnormal in *mbk-2* mutants, consistent with genetic evidence that *mbk-2* has other functions and with the requirement of *mbk-2* activity at the one-cell stage. We propose that *mbk-2* potentiates the degradation of MEI-1 and other proteins, possibly via direct phosphorylation.

EMBO reports **4**, 1175–1181 (2003)
doi:10.1038/sj.embor.7400029

INTRODUCTION

Microtubule (MT) functions are largely influenced by dynamic instability. Modulation of MT dynamics is thought to allow redistribution of MTs during the cell cycle and development, and there is considerable interest in identifying novel modulating proteins. During the first cell division of *Caenorhabditis elegans* embryos, pronuclear migration and positioning of the mitotic spindle require an intact MT cytoskeleton (Strome & Wood, 1983). These MT-based processes are known to be affected by several classes of proteins, among which are tubulins and their cofactors (Gonczy *et al.*, 2000), the dynein/dynactin motor complex (Skop & White, 1998; Gonczy *et al.*, 1999), the XMAP215/Dis1 family member ZYG-9 (Matthews *et al.*, 1998) and its binding partner TAC-1 (Bellanger & Gonczy, 2003; Srayko *et al.*, 2003) and the MT-severing protein MEI-1/katanin (Srayko *et al.*, 2000). MEI-1 activity is required only for meiotic spindle function, but ectopic mitotic expression results in short MTs (Clark-Maguire & Mains, 1994). It was shown that the postmeiotic inactivation of MEI-1 requires the Nedd8 ubiquitin-like conjugation pathway (Kurz *et al.*, 2002; Pintard *et al.*, 2003a). By screening for mutants affecting the first cell division, we sought to identify novel genes required for MT growth and to define the pathways in which they are involved. Here we report the study of *mbk-2*, a gene required for MEI-1 inactivation.

[1]Max-Planck-Institute of Molecular Cell Biology and Genetics, Pfotenhauerstrasse 108, D-01307 Dresden, Germany
[2]Genes and Development Research Group, Department of Biochemistry & Molecular Biology, University of Calgary, 3330 Hospital Drive NW, Calgary, Alberta, Canada T2N 4N1
[+]Corresponding author. Tel: +49 351 210 1700; Fax: +49 351 210 1289; E-mail: hyman@mpi-cbg.de

Received 13 August 2003; revised 8 October 2003; accepted 8 October 2003
Published online 21 November 2003

RESULTS AND DISCUSSION

mbk-2 is required maternally for MT-dependent processes

The *dd5ts* temperature-sensitive (ts) mutation was isolated in a screen for maternal-effect lethal mutants affecting the first cell division. *dd5ts* is a strict maternal and fully recessive allele at 25 °C (see Methods). Hereafter, we refer to embryos from homozygous *dd5ts* hermaphrodites grown at 25 °C as *dd5ts* embryos or *dd5ts* mutants. Analysis of *dd5ts* mutants by differential interference contrast (DIC) microscopy revealed pronuclear migration defects and aberrant spindle positioning: the spindle always forms before pronuclear meeting in the posterior of the embryo, along its short axis (Fig. 1A). In contrast, meiosis appears normal in *dd5ts* embryos as judged by the presence of a single female pronucleus ($n = 27$). This was additionally confirmed by the presence of two GFP$^+$ polar bodies in a *dd5ts*; histone::GFP background (see below, $n = 10$). Failure of pronuclear migration and establishment of a transverse spindle are indicative of MT defects, a phenotype also observed after treatment with low doses of the MT-depolymerizing drug nocodazole (Strome & Wood, 1983). We confirmed the presence of MT defects in *dd5ts* mutants by immunostaining for α-tubulin (Fig. 1B): astral MT extended 11.3 and 6.6 μm from the

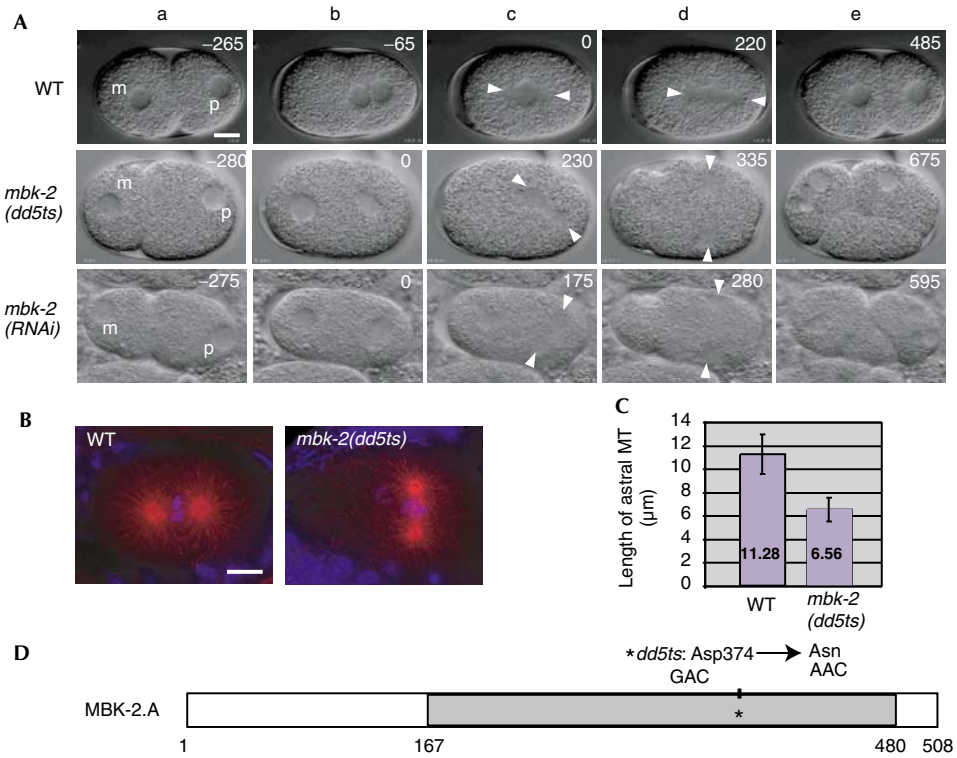

Fig. 1 | *mbk-2* encodes a serine/threonine kinase required for microtubule-based processes in the one-cell *Caenorhabditis elegans* embryo. (**A**) Time-lapse differential interference contrast series from recordings of wild-type (WT), *mbk-2(dd5ts)* and *mbk-2(RNAi)* embryos. In this and subsequent figures, anterior is to the left and the bar represents 10 μm. Time (s) is relative to nuclear envelope breakdown (NEB). (**a**) Maternal (m) and paternal (p) pronuclei at opposite sides of the cell. (**b**,**c**) In WT, pronuclei meet before NEB ($t = 0$) whereas the male pronucleus undergoes NEB and sets up the spindle before pronuclear meeting in *mbk-2(−)*. In most cases, the maternal pronucleus is eventually captured by the spindle (32/37 in *dd5ts*; 14/15 in *RNAi* embryos). (**d**) Unlike WT, the spindle forms transversely in the posterior in *mbk-2(−)*. Arrowheads indicate spindle poles. (**e**) At the two-cell stage, multiple nuclei and ectopic furrows are visible in *mbk-2(−)*. (**B**) Fixed embryos stained for α-tubulin (red) and DNA (blue) at prometaphase in WT and *mbk-2(dd5ts)*. The spindle axis is transverse and MTs less frequently reach the cellular cortex in *mbk-2(dd5ts)*. (**C**) Average length of astral MTs in WT and *mbk-2(dd5ts)*. MTs were visualized as in (**B**). The ten longest MTs from each centrosome were measured in five embryos of each genotype. (**D**) Schematic structure of the MBK-2.A protein. The grey box indicates the serine/threonine kinase domain, where the *dd5ts* mutation is located (asterisk).

centrosome in wild-type (WT) and *dd5ts* embryos, respectively (Fig. 1C).

mbk-2 encodes a serine/threonine kinase

To determine the molecular identity of *dd5ts*, we mapped it to +7.1 map units on chromosome IV (see Methods). By analysing the DIC phenotypes of all genes in this region from a genome-wide RNAi screen (Soennichsen *et al.*, unpublished data), we found that RNAi of the predicted gene F49E11.1 showed a pronuclear migration phenotype similar to *dd5ts* ($n = 15$). We identified a missense (Asp to Asn) mutation in F49E11.1 (Fig. 1D) and confirmed the gene identity by performing cosmid rescue of the mutant (see Methods). The similarity between the *dd5ts* and the RNAi phenotypes and the fact that the null allele *mbk-2(pk1427)* generated by Raich *et al.* (2003) and analysed by Pellettieri *et al.* (2003) displays a similar one-cell phenotype suggests that *dd5ts* is a strong loss-of-function mutation of *mbk-2*.

This gene was previously named *mbk-2* based on its homology to the *Drosophila minibrain kinase* gene (Raich *et al.*, 2003). It encodes a conserved serine/threonine kinase (sharing 73 and 67% identity with human DYRK2 and DYRK3 respectively, and 45% with *Schizosaccharomyces pombe* Pom1). *mbk-2* has three predicted splice variants that differ mostly in amino-termini; the *dd5ts* mutation in the carboxy-terminal kinase domain affects all three forms. The Asp residue altered by the mutation is conserved among all homologues examined, suggesting that it is crucial for the function of all family members.

Centrosome organization is unaffected in *mbk-2* mutants

MT-based defects can arise from defects in centrosomes (Hannak *et al.*, 2002) or in MT growth (Matthews *et al.*, 1998; Srayko *et al.*, 2003). To assess the basis of the MT defects in *mbk-2(dd5ts)*, we first assayed the presence of centrosomal markers using a strain expressing γ-tubulin::GFP and histone::GFP in the *mbk-2(dd5ts)* background. In all time-lapse movies, we observed no difference in the γ-tubulin::GFP signal in mutants compared to WT (Fig. 2A, $n = 12$). Similar results were obtained using a line expressing TAC-1::GFP (Fig. 2B, $n = 5$). Likewise, we did not detect any difference in the expression of the ZYG-9 protein in fixed WT and *mbk-2*

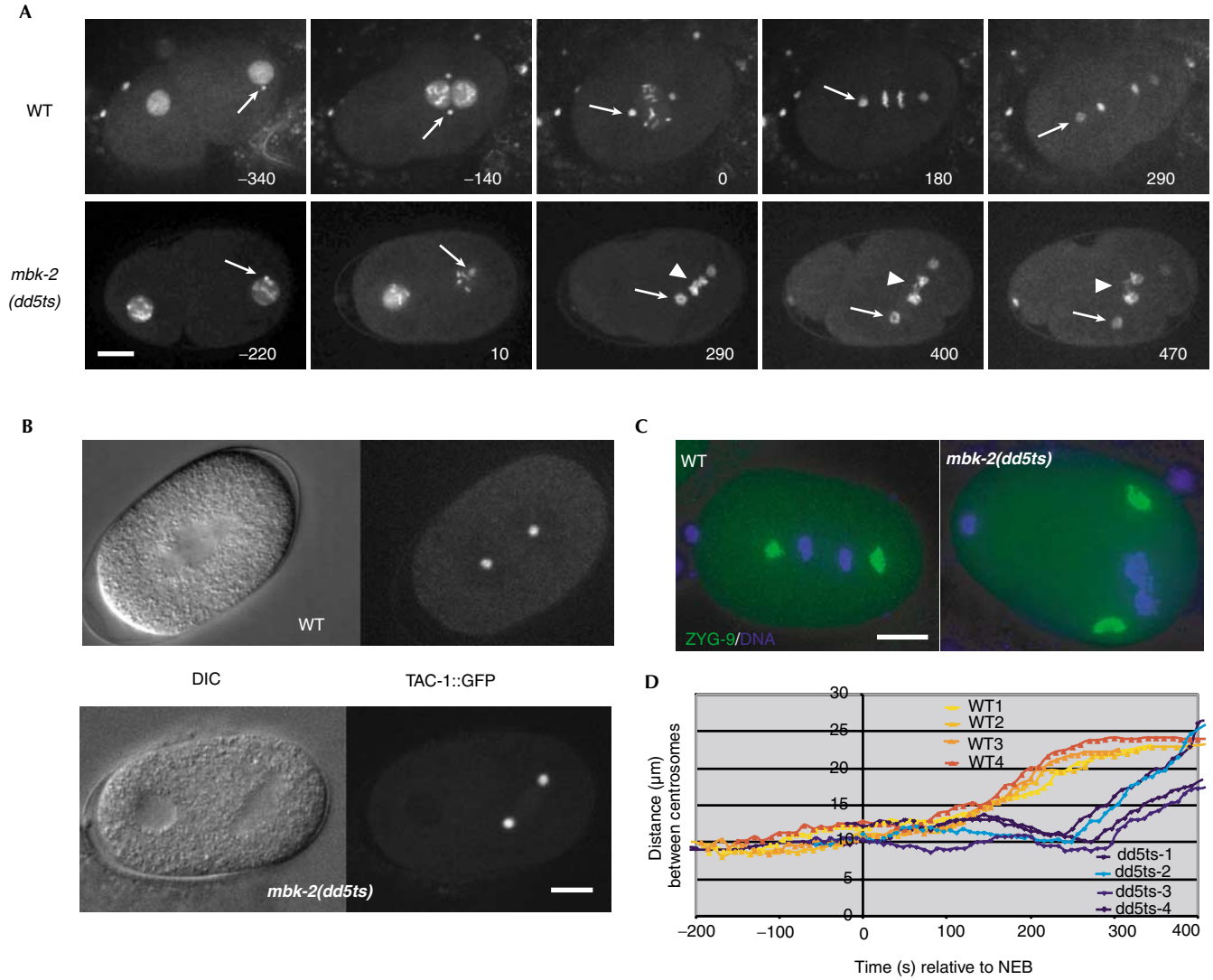

Fig. 2|Centrosome organization is normal in *mbk-2* mutants but chromosome segregation is impaired. (**A**) Time-lapse GFP series from four-dimensional analyses of wild-type (WT) and *mbk-2(dd5ts)* embryos expressing histone and γ-tubulin::GFP. Time (s) is relative to nuclear envelope breakdown (NEB). Embryos are shown at corresponding stages to those in Fig. 1A. In the mutant, centrosome labelling (arrows) appears unchanged, but lagging chromosomes are visible from early anaphase to the two-cell stage (arrowheads). (**B**) Snapshots taken shortly after NEB from time-lapse recordings of WT and *mbk-2(dd5ts)* embryos expressing TAC-1::GFP. The mutant shows normal GFP expression. (**C**) Late-anaphase embryos stained for ZYG-9 (green) and DNA (blue). In the mutant, ZYG-9 expression is unaffected, but a failure in chromosome segregation is visible. (**D**) Distance between centrosomes (µm) in one-cell embryos versus time, observed in embryos expressing γ-tubulin::GFP as shown in (**A**). Four embryos per genotype were tracked. DIC, differential interference contrast.

embryos (Fig. 2C, $n=17$). To assess further the defect in *mbk-2* mutants, we plotted the distance between centrosomes during the first cell division (Fig. 2D). We observed that centrosomes separated around the male pronucleus during pronuclear migration as in WT (before nuclear envelope breakdown (NEB)). We did not see a collapse of spindle poles prior to anaphase as is observed in *zyg-9(RNAi)* embryos (Srayko *et al.*, 2003). Interestingly, we found that anaphase onset, as determined by chromosome segregation, was delayed by >100 s in mutant embryos ($n=4$), suggesting that loss of *mbk-2* could activate a spindle checkpoint (Kitagawa & Rose, 1999). We concluded that centrosome separation and maturation are normal in *mbk-2* mutants at the one-cell stage.

In our initial DIC recordings, we consistently observed multiple nuclei of variable size at the two-cell stage even though meiosis appeared normal. To check whether this phenotype could be due to a chromosome segregation failure, we followed chromosomes in living embryos using histone::GFP. We reproducibly observed chromosome bridges at anaphase (Fig. 2A, in 12 out of 14 embryos). We also examined DNA in fixed embryos (Fig. 2C) and

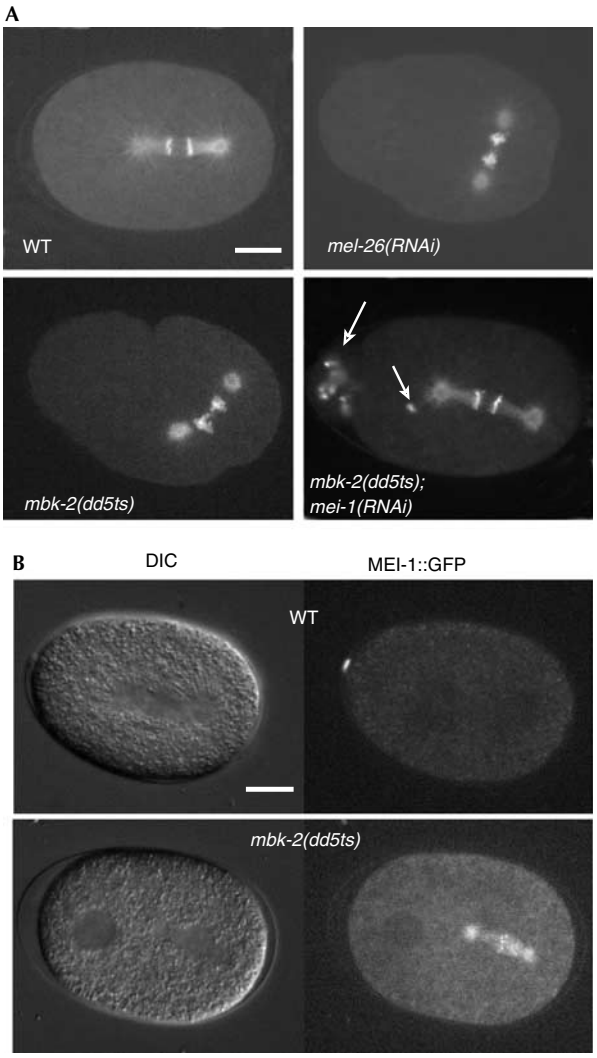

Fig. 3 | *mbk-2* microtubule defects result from persistence of MEI-1/katanin during mitosis. (**A**) Images from time-lapse movies of wild-type (WT), *mel-26(RNAi)*, *mbk-2(dd5ts)* and *mbk-2(dd5ts); mei-1(RNAi)* anaphase embryos expressing histone::GFP and β-tubulin::GFP. Note the similarity between *mel-26(RNAi)* and *mbk-2(dd5ts)* embryos, which both exhibit abnormal spindle positioning and lagging chromosomes. These defects are entirely suppressed in *mei-1(RNAi); mbk-2(dd5ts)* embryos (bottom, right panel in **A**). Enlargement of the polar body indicates a meiosis failure in these embryos (left arrow), characteristic of *mei-1(RNAi)*. The arrow at the right points to meiotic chromosomes that have been abnormally captured by the microtubules. (**B**) WT and *mbk-2(dd5ts)* early-anaphase embryos expressing MEI-1::GFP. The corresponding differential interference contrast (DIC) images are shown to the left. Note the presence of ectopic MEI-1::GFP on the spindle in the mutant.

could detect lagging chromosomes at anaphase in 73% of the *mbk-2* embryos ($n = 48$). In contrast, we did not detect any chromosome segregation defects in *zyg-9(b244)* embryos, which also exhibit short MTs ($n = 21$). Therefore, this failure of segregating chromosomes was specific to *mbk-2* rather than due to a general MT phenotype.

Ectopic MEI-1/katanin causes MT defects in *mbk-2* mutants

The above experiments suggest that the MT phenotype in *mbk-2* mutants is not due to a centrosome defect. It also differs from the Zyg-9 phenotype (Matthews *et al.*, 1998; Srayko *et al.*, 2003) in at least three ways: chromosome segregation is affected while meiosis and spindle MTs are not. Rather, the Mbk-2 phenotype is reminiscent of loss-of-function phenotypes of the *mel-26* gene (see *mel-26(RNAi)*, Fig. 3A), the activity of which is required for the postmeiotic inactivation of MEI-1/katanin MT-severing complex (Dow & Mains, 1998). We asked whether the Mbk-2 MT-related phenotype could be due to the ectopic mitotic activity of MEI-1. To investigate this, we examined the effect of depleting MEI-1 activity by RNAi in *mbk-2(dd5ts)* mutants (Fire *et al.*, 1998). Time-lapse recordings showed that the pronuclear migration, spindle positioning and chromosome segregation defects were suppressed in 100% of the *mbk-2(dd5ts); mei-1(RNAi)* embryos (DIC, $n = 25$; histone::GFP; β-tubulin::GFP, $n = 10$; Fig. 3A). A confirmation that *mei-1* was inactivated in these embryos came from the observation that all displayed striking enlargement of the polar body, a hallmark of *mei-1* loss-of-function mutants, which results from meiotic spindle defects (Mains *et al.*, 1990). We did not see rescue of the *mbk-2*-induced lethality, presumably because of this meiotic failure. We conclude that the inactivation of the *mei-1* function is sufficient to suppress all *mbk-2(dd5ts)* MT-related phenotypes in the one-cell embryo. This suggests that MEI-1 is ectopically present in *mbk-2* mutants. To test this, we examined the distribution of MEI-1::GFP in *mbk-2* embryos. Unlike WT embryos, where residual MEI-1::GFP is present only in the polar bodies during mitosis, we observed that MEI-1::GFP was ectopically present on the spindle and on chromosomes

Table 1 | *mbk-2* synergizes with mutations in the *mei-1* pathway

Genotype	Hatching rate at 20 °C
mbk-2(dd5ts)	56
mbk-2(dd5ts)/+	98
mel-26(ct61)/+	46
mel-26(ct61)/+; mbk-2(dd5ts)/+	25
mel-26(ct61)/+; mbk-2(dd5ts)	1
mei-1(ct46)/+	21
mei-1(ct46)/+; mbk-2(dd5ts)/+	9.4
mei-1(ct46)/+; mbk-2(dd5ts)	0.2
tbb-2(sb26)	98
mbk-(dd5ts); tbb-2(sb26)	82
	Hatching rate at 25 °C
mbk-2(dd5ts)	2
mei-1(ct46)	0*
tbb-2(sb26)	97*
mei-1(ct46); tbb-2(sb26)	67*
mbk-(dd5ts); tbb-2(sb26)	0

Percentage of living larvae in the progeny of animals of the indicated genotype ($n > 400$ in all cases). *Lu *et al.* (2003).

throughout the first cell cycle in all *mbk-2* embryos (Fig. 3B, $n = 20$). We conclude that the WT activity of MBK-2 prevents the mitotic persistence of MEI-1.

Consistent with these observations, we found that *mbk-2* interacts genetically with mutations in the *mei-1* pathway. The ts semidominant *mei-1(ct46)* and *mel-26(ct61)* mutations result in ectopic MEI-1 (Clark-Maguire & Mains, 1994; Dow & Mains, 1998) but allowed respectively 21 and 46% hatching as heterozygotes at the semipermissive temperature of 20 °C. However, when combined with *mbk-2(dd5ts)*, which itself showed 56% hatching under these conditions, the resulting double mutants had ≤1% hatching, indicating a strong enhancement of the defects (Table 1). Likewise, *tbb-2(sb26)*, a mutation in the β-tubulin gene that interferes with MEI-1 activity (Lu *et al.*, 2003), decreased the lethality caused by *mbk-2* under semipermissive conditions, indicating that a proportion of the *mbk-2* lethality is indeed caused by ectopic MEI-1 expression. Furthermore, at 25 °C, *tbb-2(sb26)* is a good suppressor of *mei-1(ct46)* but not of *mbk-2(dd5ts)* (67% hatching in *ct46; sb26* versus 0% in *dd5ts; sb26*), indicating that *mbk-2* has essential targets other than *mei-1*. Together, these results indicate that *mbk-2* acts in the *mel-26* pathway and that *mbk-2* has functions other than downregulating MEI-1.

mbk-2 is required for the proper segregation of P granules

We sought to determine the additional functions of *mbk-2* suggested by the genetic data. The terminal DIC phenotype of *mbk-2* mutants revealed that cells are able to divide and differentiate, but embryos never undergo morphogenesis; most seem to have excess pharyngeal cells abnormally located on the external surface and lack hypodermal cells. This late patterning defect could be due to an earlier polarity phenotype (Bowerman, 1998). To determine at which stage this defect arises, we performed temperature shift experiments. We did not detect a requirement for MBK-2 in late embryogenesis or in larval development. When embryos reared at the permissive temperature (16 °C) were shifted to the restrictive temperature (25 °C), two-cell embryos hatched (14 out of 15) whereas most of the one-cell stage embryos died (21 out of 24). Conversely, in temperature downshift experiments, all embryos died ($n = 60$), including those that were shifted during pronuclear migration in the one-cell stage ($n = 17$). Together with the fact that *mbk-2* does not seem to be required during meiosis (see above), these data are consistent with a requirement of *mbk-2* during the one-cell stage.

To examine potential defects at the one-cell stage, we monitored the expression of several polarity markers, including P granules and PAR proteins. P granules are germline determinants; they segregate to the posterior pole of the zygote and subsequently to the germline blastomeres (Strome & Wood, 1982). We observed that P granules fail to localize properly in *mbk-2* mutants, whereas *zyg-9* mutants and *mel-26(RNAi)* embryos show a WT pattern (Fig. 4A). Therefore, this defect is not due to the misplaced spindle *per se*. Since *mel-26(RNAi)* and *mbk-2* mutant embryos both exhibit ectopic MEI-1, this suggests that *mbk-2* specifically affects P-granule distribution independently of acting on MEI-1. This was further confirmed by the failure of *mei-1(RNAi)* to suppress the P-granule localization defect in *mbk-2* mutants (Fig. 4A). We also followed the expression of the cortical markers PAR-2::GFP (posterior) and PAR-6::GFP (anterior) in living embryos. Interestingly, we found no difference in the dynamic distribution of these markers between *mbk-2* and WT (Fig. 4B). PAR-1 protein distribution in *mbk-2* fixed embryos was also normal (not shown, $n = 8$). In conclusion, *mbk-2* activity is necessary for the proper localization of the P granules but dispensable for the distribution of at least three cortical polarity markers.

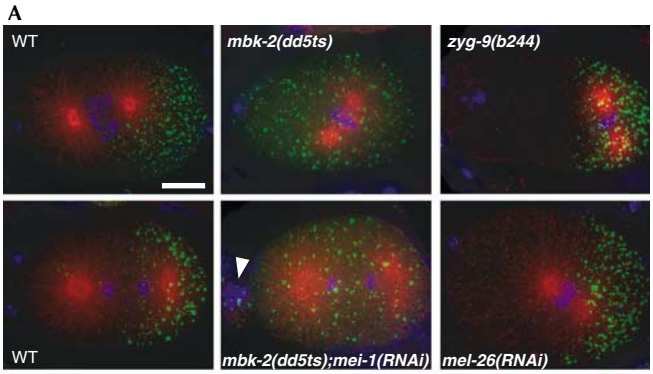

P-granules localization	Posterior	Partially posterior	Evenly distributed
WT	34	0	0
mbk-2(dd5ts)	0	9	65
mbk-2(RNAi)	0	0	11
zyg-9(b244)	19	0	0
mbk-2(dd5ts); mei-1(RNAi)	0	2	15
mel-26(RNAi)	16	0	0

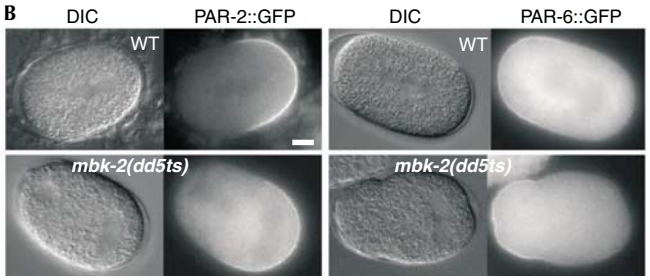

Fig. 4 | *mbk-2* activity is required for the proper localization of P granules. (**A**) Fixed embryos stained for microtubules (red), DNA (blue) and P granules (anti-PGL-1, green), in wild-type (WT), *mbk-2(dd5ts)*, *zyg-9(b244)*, *mel-26(RNAi)* and *mbk-2(dd5ts); mei-1(RNAi)* embryos. The arrowhead points to the enlarged polar body due to meiotic failure in the latter. The table shows the number of embryos of each genotype with a given type of P-granule distribution. (**B**) WT and *mbk-2(dd5ts)* embryos expressing PAR-2::GFP and PAR-6::GFP. The distribution of the cortical markers is unaffected in the mutant. DIC, differential interference contrast.

Conclusion

Our results show that *mbk-2* activity is essential in the *C. elegans* zygote to ensure the postmeiotic inactivation of the MT-severing

protein MEI-1. MEI-1 inactivation requires the Nedd8 ubiquitin-like conjugation pathway (Kurz *et al.*, 2002), through neddylation and deneddylation of the CUL-3 E3 ligase (Pintard *et al.*, 2003a). MEL-26 is part of the CUL-3 complex and is proposed to function as a substrate-specific adaptor for MEI-1 (Pintard *et al.*, 2003b; Xu *et al.*, 2003). In the well-characterized yeast Skp1–Cullin–F-box protein (SCF) complex, target phosphorylation is a prerequisite for recognition and subsequent degradation by the E3 ligase (reviewed in Pickart, 2001). By analogy—although the mechanism used by CUL-3 to recognize substrates such as MEI-1 is unknown—we suggest the possibility that *mbk-2* could phosphorylate MEI-1, specifying it for degradation. It is likely that *mbk-2* controls the destruction of other proteins, such as those required for correct P-granule segregation. In an elegant study, Pellettieri *et al.* (2003) recently reported that *mbk-2* is also required for the degradation of the germline protein PIE-1 in anterior blastomeres. These authors further demonstrate that *mbk-2* is nevertheless not a general activator of protein degradation. Therefore, it seems likely that *mbk-2* regulates the phosphorylation state of specific proteins as a signal for their recognition by the proteasome. This would provide a link between protein kinase signalling and the control of protein turnover in the one-cell embryo.

METHODS

Strains, alleles and genetic analysis. *C. elegans* culture, mutagenesis and meiotic mapping were performed using standard techniques (Brenner, 1974). N2 Bristol was the WT strain. The following alleles were used: LGI: *dpy-5(e61)*, *mei-1(ct46)*, *mel-26(ct61)*, *unc-29(e1072)*; LGII: *rol-6(e187)*, *zyg-9(b244ts)*; LGIII: *unc-32(e189)*, *tbb-2(sb26)*; LGIV: *unc-5(e53)*, *unc-31(e169)*, *dpy-4(e1166)*, *dpy-20(e1282)*; LGV: *dpy-11(e224)*; LGX: *lon-2(e678)*. The *dd5ts* allele was isolated in a screen for maternal-effect lethal mutations after ethylmethane sulphonate (EMS) mutagenesis, in which F_2 worms were cultured individually (six-well format) and their progeny scored for viability. Only plates that contained dead eggs in at least one well were kept and examined for one-cell embryo phenotypes. *dd5ts* was back-crossed five times, giving rise to TH20. At the permissive temperature of 16 °C, homozygous *dd5ts* hermaphrodites produced 90% viable embryos ($n = 829$); at the restrictive temperature of 25 °C, 98% of embryos died ($n = 460$). *dd5ts* is recessive: *dd5ts*/+ had 99% living progeny at 25 °C ($n = 262$). Paternal requirement was excluded since *dd5ts* homozygous males had viable progeny when mated to *fog-2(q71)* females ($n > 300$). Genetic interactions with *mei-1* pathway genes were performed as described by Mains *et al.* (1990), by collecting complete broods from four or more hermaphrodites.

Mapping gave the following results: *unc-31* (12/91) *dd5ts* (79/91) *dpy-4*, which placed *dd5ts* at +7.1 on LGIV. T13E8 cosmid DNA (30 ng μl^{-1}), which contains the F49E11.1 predicted gene, was mixed with pRF4 carrying the dominant marker *rol-6(su1006)* (150 ng μl^{-1}) and injected into TH20 as in Mello *et al.* (1991). This rescued the *dd5ts* maternal-effect lethality at 25 °C in 4 out of 8 transgenic lines.

The GFP strains used were TH30 (γ-tubulin::GFP; histone::GFP), TH14 (TAC-1::GFP), XA3501 (β-tubulin::GFP; histone::GFP), a gift from I. Mattaj, EU1065 (MEI-1::GFP) received from B. Bowerman, JH1380 (PAR-2::GFP) provided by G. Seydoux, and TH25 (PAR-6::GFP). TH20 was crossed to all of them to generate homozygous *dd5ts*; GFP marker.

RNA interference, immunofluorescence and microscopy. RNAi experiments and immunostaining of ZYG-9, P granules, α-tubulin (DM1α, Sigma) and PAR-1 were performed as described (Oegema *et al.*, 2001). Image acquisition of embryos as well as MT measurements were performed as in Srayko *et al.* (2003). For four-dimensional movies of GFP strains, embryos were observed on a spinning disc confocal microscope. Three focal planes were acquired at 1 μm intervals every 10 s.

ACKNOWLEDGEMENTS

We thank S. Strome for the P-granule antibody, and C. Cowan, C. Hoege, E. Marois, M. Srayko and W. Zachariae for suggestions on the manuscript. Some strains were supplied by the Caenorhabditis Genetics Center. We also thank Cenix BioScience GmbH for access to the RNAi database, and K. Oegema for sharing unpublished data and for generating TH30. S.Q. was supported by a Marie Curie Fellowship from the EC, and P.E.M. by grants from the Canadian Institutes of Health Research (CIHR) and the Alberta Heritage Foundation for Medical Research.

REFERENCES

Bellanger, J.M. & Gonczy, P. (2003) TAC-1 and ZYG-9 form a complex that promotes microtubule assembly in *C. elegans* embryos. *Curr. Biol.*, **13**, 1488–1498.

Bowerman, B. (1998) Maternal control of pattern formation in early *Caenorhabditis elegans* embryos. *Curr. Top. Dev. Biol.*, **39**, 73–117.

Brenner, S. (1974) The genetics of *Caenorhabditis elegans*. *Genetics*, **77**, 71–94.

Clark-Maguire, S. & Mains, P.E. (1994) Localization of the *mei-1* gene product of *Caenorhaditis elegans*, a meiotic-specific spindle component. *J. Cell Biol.*, **126**, 199–209.

Dow, M.R. & Mains, P.E. (1998) Genetic and molecular characterization of the *Caenorhabditis elegans* gene, *mel-26*, a postmeiotic negative regulator of *mei-1*, a meiotic-specific spindle component. *Genetics*, **150**, 119–128.

Fire, A., Xu, S., Montgomery, M.K., Kostas, S.A., Driver, S.E. & Mello, C.C. (1998) Potent and specific genetic interference by double-stranded RNA in *Caenorhabditis elegans*. *Nature*, **391**, 806–811.

Gonczy, P., Pichler, S., Kirkham, M. & Hyman, A.A. (1999) Cytoplasmic dynein is required for distinct aspects of MTOC positioning, including centrosome separation, in the one cell stage *Caenorhabditis elegans* embryo. *J. Cell Biol.*, **147**, 135–150.

Gonczy, P. *et al.* (2000) Functional genomic analysis of cell division in *C. elegans* using RNAi of genes on chromosome III. *Nature*, **408**, 331–336.

Hannak, E., Oegema, K., Kirkham, M., Gonczy, P., Habermann, B. & Hyman, A.A. (2002) The kinetically dominant assembly pathway for centrosomal asters in *Caenorhabditis elegans* is γ-tubulin dependent. *J. Cell Biol.*, **157**, 591–602.

Kitagawa, R. & Rose, A.M. (1999) Components of the spindle-assembly checkpoint are essential in *Caenorhabditis elegans*. *Nature Cell Biol.*, **1**, 514–521.

Kurz, T., Pintard, L., Willis, J.H., Hamill, D.R., Gonczy, P., Peter, M. & Bowerman, B. (2002) Cytoskeletal regulation by the Nedd8 ubiquitin-like protein modification pathway. *Science*, **295**, 1294–1298.

Lu, C., Srayko, M. & Mains, P.E. (2003) The *C. elegans* microtubule severing complex MEI-1/MEI-2 katanin interacts differently with two superficially redundant β-tubulin isotypes. *Mol. Biol. Cell* (in the press).

Mains, P.E., Kemphues, K.J., Sprunger, S.A., Sulston, I.A. & Wood, W.B. (1990) Mutations affecting the meiotic and mitotic divisions of the early *Caenorhabditis elegans* embryo. *Genetics*, **126**, 593–605.

Matthews, L.R., Carter, P., Thierry-Mieg, D. & Kemphues, K. (1998) ZYG-9, a *Caenorhabditis elegans* protein required for microtubule organization and function, is a component of meiotic and mitotic spindle poles. *J. Cell Biol.*, **141**, 1159–1168.

Mello, C.C., Kramer, J.M., Stinchcomb, D. & Ambros, V. (1991) Efficient gene transfer in *C. elegans*: extrachromosomal maintenance and integration of transforming sequences. *EMBO J.*, **10**, 3959–3970.

Oegema, K., Desai, A., Rybina, S., Kirkham, M. & Hyman, A.A. (2001) Functional analysis of kinetochore assembly in *Caenorhabditis elegans*. *J. Cell Biol.*, **153**, 1209–1226.

Pellettieri, J., Reinke, V., Kim, S.K. & Seydoux, G. (2003) Coordinate activation of maternal protein degradation during the egg-to-embryo transition in *C. elegans*. *Dev. Cell*, **5**, 451–462.

Pickart, C.M. (2001) Mechanisms underlying ubiquitination. *Annu. Rev. Biochem.*, **70**, 503–533.

Pintard, L., Kurz, T., Glaser, S., Willis, J.H., Peter, M. & Bowerman, B. (2003a) Neddylation and deneddylation of CUL-3 is required to target MEI-1/katanin for degradation at the meiosis-to-mitosis transition in *C. elegans*. *Curr. Biol.*, **13**, 911–921.

Pintard, L. *et al.* (2003b) The BTB protein MEL-26 is a substrate-specific adaptor of the CUL-3 ubiquitin-ligase. *Nature*, **425**, 311–316.

Raich, W.B., Moorman, C., Lacefield, C.O., Lehrer, J., Bartsch, D., Plasterk, R.H., Kandel, E.R. & Hobert, O. (2003) Characterization of *Caenorhabditis elegans* homologs of the Down syndrome candidate gene DYRK1A. *Genetics*, **163**, 571–580.

Skop, A.R. & White, J.G. (1998) The dynactin complex is required for cleavage plane specification in early *Caenorhabditis elegans* embryos. *Curr. Biol.*, **8**, 1110–1116.

Srayko, M., Buster, D.W., Bazirgan, O.A., McNally, F.J. & Mains, P.E. (2000) MEI-1/MEI-2 katanin-like microtubule severing activity is required for *Caenorhabditis elegans* meiosis. *Genes Dev.*, **14**, 1072–1084.

Srayko, M., Quintin, S., Schwager, A. & Hyman, A.A. (2003) *Caenorhabditis elegans* TAC-1 and ZYG-9 form a complex that is essential for long astral and spindle microtubules. *Curr. Biol.*, **13**, 1506–1511.

Strome, S. & Wood, W.B. (1982) Immunofluorescence visualization of germ-line-specific cytoplasmic granules in embryos, larvae, and adults of *Caenorhabditis elegans*. *Proc. Natl Acad. Sci. USA*, **79**, 1558–1562.

Strome, S. & Wood, W.B. (1983) Generation of asymmetry and segregation of germ-line granules in early *C. elegans* embryos. *Cell*, **35**, 15–25.

Xu, L., Wei, Y., Reboul, J., Vaglio, P., Shin, T.H., Vidal, M., Elledge, S.J. & Harper, J.W. (2003) BTB proteins are substrate-specific adaptors in an SCF-like modular ubiquitin ligase containing CUL-3. *Nature*, **425**, 316–321.